JOURNAL OF Applied Polymer SCIENCE

Preparation and Properties of Porous L-Tryptophan Imprinted Latex Membrane from Core-Shell Emulsion

Meina Lin, Xiao Li, Weiying Zhang, Xiaoguang Ying
College of Chemistry and Chemical Engineering, Fuzhou University, Fuzhou 350108, China

Correspondence to: X. Li (E-mail: lxzwy@fzu.edu.cn)

ABSTRACT: Molecularly imprinted latex membrane (MILM) is prepared by core-shell emulsion technique in the presence of a template molecule (L-Tryptophan). A hard inward and soft outward microstructure latex particle is designed to obtain MILM with both flexibility and impact strength. Molecularly imprinted layer with high crosslinking degree is grafted on the surface of core-shell latex particles. NaCl, glucose, urea, polyethylene glycol, M_w 300, etc., are added during the film-forming process to produce porous microstructure in MILM. Fourier transform infrared spectroscopy (FTIR) and Scatchard analysis are used to investigate the interaction between L-Tryptophan and MILM and the binding ability of the resultant MILM, respectively. The functional binding and separation performances in aqueous medium towards template are carried out. The results reveal that the content and type of porogen and the shell composition have significant effects on adsorption capacity and separation ability. MILM with glucose as porogen shows high recognition towards the template with adsorption separation factor reaching 9.06. © 2012 Wiley Periodicals, Inc. J. Appl. Polym. Sci. 000: 000–000, 2012

KEYWORDS: molecular imprinting; membranes; core-shell emulsion; separation techniques; selectivity; L-Tryptophan

Received 15 February 2012; accepted 21 March 2012; published online
DOI: 10.1002/app.37750

INTRODUCTION

Molecularly imprinted membrane (MIM) has received increasing attention due to its merits of high selective binding to the template and easy operation. A simple preparation of MIM is carried out by the copolymerization of functional monomer and crosslinker in the presence of a template molecule. After removing the template, a three dimensional network of porous thin film containing cavities ideally shaped for template is obtained.[1]

MIM was first prepared by Piletsky[2] in 1990 via *in situ* bulk polymerization of acrylate monomers. After that, the application of molecular imprinting technique to separating membrane was developed rapidly. However, MIM prepared via this method[3,4] had poor mechanical stability due to the high crosslinkage and the swollen structure,[5] and had low membrane permeability due to the low porosity. Another approach for synthesis of MIM was phase inversion method. Yoshikawa et al.[6,7] and Kobayashi et al.[8,9] introduced the molecular memory of template into the membrane via dry and wet phase inversion process, respectively. Despite their good mechanical stability and recognition properties, these MIMs were not stable in organic environment. On the other hand, the process of preparing MIM was complicated due to the contradiction between the conditions required for the formation of molecularly imprinted sites and the control of pore structure.[2] In addition, a large quantity of solvent was needed. Yet another significant approach to synthesize MIM was proposed by surface modification of commercially available microporous membranes. The surface functionalization technique included surface grafting by photopolymerization[10–12] and surface coating by thermal polymerization.[13–15] This method had the advantage of adjusting the pore structure of membrane and the recognition of molecularly imprinted polymer (MIP) simultaneously by two different materials, but its operation was complicated and the procedure was tedious.

The aim of the present research is to develop a novel method for preparation of self-supported molecularly imprinted latex membrane (MILM). The procedure of MILM preparation contains the synthesis of core-shell emulsion with a thin molecularly imprinted layer and the film-formation from the molecularly imprinted emulsion in the presence of porogen. This kind of self-supported MILM has several advantages. First, the mechanical stability of MILM can be adjusted by changing the composition of core-shell latex particles. In this study, the latex particles with hard inward and soft outward microstructure

were designed. The soft phase provides a lower minimum film-forming temperature to emulsion and leads to a good flexibility, whereas the hard phase contributes to good impact strength. Second, after a MILM has been formed, extracting porogen (such as NaCl, glucose, urea, polyethylene glycol, etc.) from it can result in a membrane with large porosity. So, the inner structure of MILM can be easily adjusted by the change of content and type of porogen. Third, the molecularly imprinted layer is modified on the surface of core-shell latex particles before MILM formation, and the specific binding sites have enough mechanical strength to protect themselves from being destroyed during the process of MILM formation. So, MILM prepared through this method coordinates membrane pore and recognition sites structure simultaneously. Additionally, this method has some other advantages, including easy operation, no pollution, and environment friendliness.

This study will investigate the influence of porogen content and type, as well as shell composition on the microscopic structure of MILM and, as a consequence, on the adsorption capacity and the permeability.

EXPERIMENTAL

Materials

L-Tryptophan (L-Trp) and L-Tyrosine (L-Tyr) were obtained from Sanland-chem International Inc. (Xiamen, China). Methyl methacrylate (MMA), butyl acrylate (BA), urea, glucose, and octylphenol polyoxyethylene ether (OP-10) were purchased from Tianjin Fuchen Chemical Reagent Plant (Tianjin, China). MMA and BA were treated by alkali washing of 5% NaOH to remove the inhibitor. Acrylamide (AM) was purchased from Yun-Jie Shanghai Chemical Reagent (Shanghai, China). Ethylene glycol dimethacrylate (EGDMA) was obtained from Fluka (Buchs, Switzerland). Potassium persulfate (KPS) was obtained from Shanghai Reagent Chemical Engineering Plant (Shanghai, China) and purified by recrystallization. Sodium dodecyl sulfonate (SLS) was purchased from China Medicine Group Shanghai Chemical Reagent Company (Shanghai, China). Polyethylene glycol M_w 300 (PEG300) was purchased from Shanghai Chemical Reagent Plant (Shanghai, China). All other reagents were used without further purification.

Synthesis of Core-Shell Emulsion

The core-shell emulsion was prepared by use of pre-emulsification technology and semi-continuous seeded emulsion polymerization method. A typical polymerization was performed in a 100 mL 3-neck flask with a magnetic agitator, a reflux cooler, a gas inlet, and a dropping funnel for the starved-feed monomer addition.

First, the flask was fed with entire amount of KPS, $NaHCO_3$, and distilled water, and purged with nitrogen for about 10 min. After that, 2 g of pre-emulsion(I) composed of 5 g MMA, 0.25 g EGDMA, and a certain amount of SLS and OP-10 was charged, then 1 mL reductant of $NaHSO_3$ was added. The mixture were stirred at 55°C. When a blue light appeared, the reaction was allowed to proceed for further 15 min to form the seeds. After that, the residual pre-emulsion(I) and $NaHSO_3$ were added under starved-feed conditions. When the addition of pre-emulsion(I) was completed, the mixture was allowed to react for 30 min at 55°C and 1 h at 65°C to form core emulsion. The preparation of PMMA/BA shell was similar to that of PMMA/EGDMA core. The second batch of KPS and $NaHCO_3$ was added for grafting MMA/BA on the PMMA/EGDMA core. Subsequently, the pre-emulsion(II) composed of 5 g monomers (including MMA and BA) and a certain amount of SLS and OP-10 was added dropwise. In some experiments, additional 0.25 g EGDMA was added in pre-emulsion(II). When the addition of pre-emulsion(II) was completed, the aging process was conducted for additional 30 min at 55°C and 1 h at 65°C.

Synthesis of Molecularly Imprinted Polymer Emulsion

The introduction of molecularly imprinted layer into the core-shell emulsion was carried out through the following procedure. First, 6 g core-shell emulsion prepared above was initially charged into a reactor as the seed, and then 6 mmol of AM (the functional monomer), 0.3 g EGDMA (the crosslinker), and 1 mmol L-Trp (the template) were added. After the temperature was raised to 55°C, the entire amount of SLS and KPS were added into the reactor. Then, the polymerization was conducted for 7 h to prepare MIP emulsion.

Preparation of Molecularly Imprinted Latex Membrane (MILM)

A certain amount of water-soluble additives (NaCl, glucose, urea, PEG300, etc.) were mixed with MIP emulsion and linear polybutyl acrylate (PBA) emulsion obtained from emulsion polymerization of butyl acrylate. Addition of PBA was effective to lower the glass transition temperature and to help form the latex film.[16] The mixture was cast into a glass mould, and then placed in a fanless laboratory oven at 50°C for 24 h. After that, some water was added into the mould for easy removal of casting MILM by careful peeling. The MILM acquired was soaked into distilled water to remove the water-soluble additives and a porous structure was obtained. The porous MILM was washed with a methanol/acetic acid (9/1, v/v) mixed solution several times to remove L-Trp until no L-Trp in the extraction solution was detected. The resultant MILM was stored in distilled water at room temperature until being used for binding experiments.

Functional Properties of MILM

Adsorption Properties. MILM (0.2 g) were placed in a 50 mL conical flask and mixed with 20 mL of 2 mmol/L L-Trp and L-Tyr mixed solution. After shaking the adsorption system at 25°C for 24 h, the residual concentration of L-Trp and L-Tyr was determined using synchronous fluorescence spectrophotometer (Cary Eclipse, Varian). The standard calibration curves for L-Trp and L-Tyr ranged from 1 to 7 μmol/L were established, respectively.

The adsorption properties of MILM, including capacity Q (μmol/g), partition coefficient K_D (mL/g), and adsorption separation factor α, were evaluated with the change of substrate concentration through the following equations:

$$Q = \frac{(C_0 - C_a) \times V}{m} \quad (1)$$

where C_0 was the initial concentration of substrates (mmol/L); C_a was the residual concentration of the substrates after

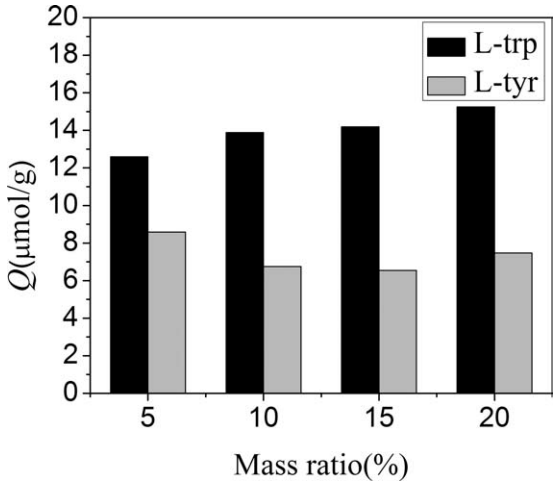

Figure 1. Effects of urea content on the adsorption capacity by MILM.

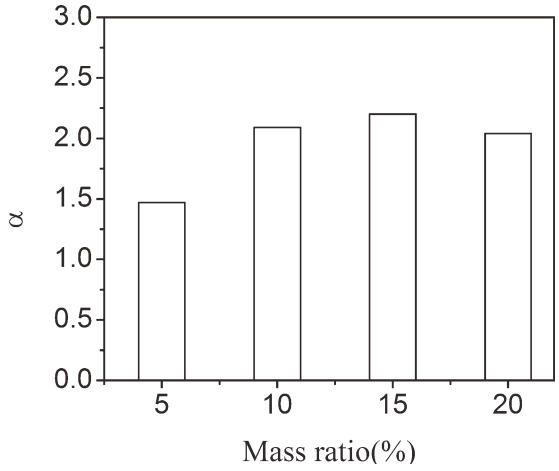

Figure 3. Effects of urea content on the separation factor by MILM.

adsorption (mmol/L); V was the volume of the initial solution (mL); and m was the weight of the MILM (g).

$$K_D = C_p/C_s \tag{2}$$

where C_p was the adsorption quantities of substrates by MILM (μmol/g); C_s was the residual concentration of substrates in the solution after adsorption (mmol/L).

$$\alpha = K_{Di}/K_{Dj} \tag{3}$$

where K_{Di} and K_{Dj} were the partition coefficients of L-Trp and L-Tyr, respectively.

Permeation Measurement. With the aim of evaluating the recognition properties of MILM toward the target molecule, permeation experiments in a permeability cell were carried out. A piece of MILM with 0.2 mm thickness was located at the interface between the two chambers of the permeability cell. 80 mL mixed solution (L-Trp and L-Tyr with initial concentration of 2 mmol/L) was added into the left chamber and 80 mL distilled water into the right one. Two chambers were stirred with magnetic stirrer at room temperature for 12 h. The concentrations of L-Trp and L-Tyr were determined simultaneously using synchronous fluorescence spectrophotometer. After permeation tests, the membranes were re-extracted with methanol/acetic acid mixed solution to regain the initial performance.

The permeation amount P (mmol/m^2) and permeation separation factor β of MILM were evaluated with the change of substrate concentration in the left chamber through the following equations:

$$P = \frac{(C_0 - C_a) \times V}{A} \tag{4}$$

$$\beta = P_i/P_j \tag{5}$$

where C_0 was the initial concentration of substrates (mmol/L); C_a was the residual concentration of the substrates (mmol/L); P_i and P_j were the permeation amount of L-Trp and L-Tyr, respectively.

Characterization of MILM

The morphologies of MILM were examined by scanning electron microscope (SEM, XL30, Philips), after breaking the MILM in the liquid nitrogen and coating the cross section with gold films. The average pore size was measured by porosity and specific surface analyzer (SSA-4200, Builder, China). The interaction between L-Try and MILM was studied by means of Fourier transform infrared spectroscopy (FTIR, Nicolet-360, Nicolet).

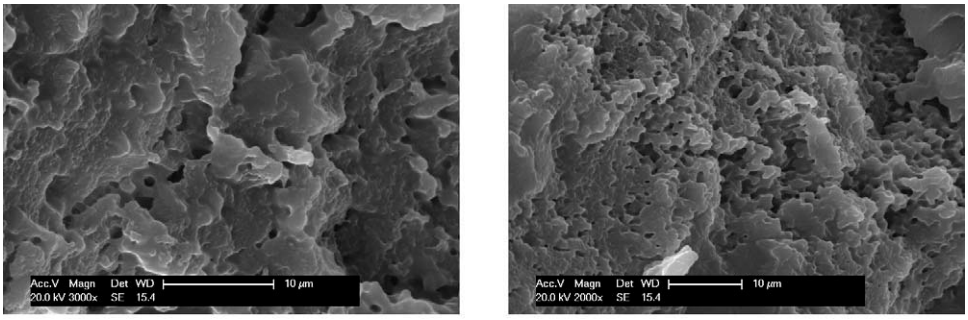

Figure 2. SEM photograph of cross-section of MILMs with (a) 10% urea, (b) 20% urea as porogen. In all of these MILMs, BA/MMA in shell composition is 4/1.

Table I. Effects of Urea Content on the Average Pore Size, Permeation Amount, and Separation Factor by MILM

Urea content (% w/w)	Average pore size (nm)	P (mmol/m^2)		β
		L-Trp	L-Tyr	
5	12.67	4.88	3.80	1.28
10	15.23	5.24	4.02	1.30
15	33.71	5.39	6.95	0.78
20	50.21	5.91	6.83	0.87

RESULTS AND DISCUSSION

Selective Binding and Separation of MILM

This self-supported MILM formed by the process of consolidation, compaction, deformation, and polymer chain inter-diffusion of latex particles[17] is compact and homogeneous. To obtain a porous membrane, a certain amount of porogen was added in the film-forming process. Further extraction of the porogen from the MILM would result in the formation of a porous film with developed inner surface.

Effects of Porogen Content

Urea was chosen to help the formation of porous microstructure in the MILM. The effects of urea content on the adsorption capability of the porous MILM are shown in Figure 1. It is demonstrated that the values of specific adsorption to L-Trp increase with the increase in the dosage of porogen. The increase in adsorption to L-Trp can be explained by the improvement of the accessibility of the L-Trp specific binding sites due to the formation of more developed inner surface caused by the increase of porogen content. As shown in Figure 2(a,b), the MILM containing more urea has higher values of the number of pores and average pore size. The values of separation factor α of MILM are presented in Figure 3. It reveals that separation factor first increases then decreases with the porogen content.

The permeation experiments in Table I indicate that the permeation amount of MILM to L-Trp and L-Tyr generally increases with the average pore size of MILM. The separation factor is beyond 1 when the content of porogen is not more than 10%, which can be explained by the preferential adsorption of the template due to affinity binding. However, the separation factor is below 1 when the content of porogen reaches 15%, which can be explained that a dramatic increase in average pore size (Table I) leads to a faster transport of non-specific substrates.

Effects of Porogen Type

Take 10% porogen content for example, a series of porogens including NaCl, glucose, urea, and PEG300 were chosen to attain porous MILMs. The influence of porogen type on the morphology of MILMs was observed. SEM analysis (Figure 4) shows that the MILMs with different types of porogen have tremendous difference in the morphology of cross section. The MILM with NaCl as porogen has large and smooth transport channels. The MILM with glucose as porogen has continuous porous structure. The MILM with urea or PEG300 as porogen has fine cavities in the inner structure, but the cavities in the former is deeper.

The influence of porogen type on the adsorption properties and separation performances of MILM were investigated. As shown

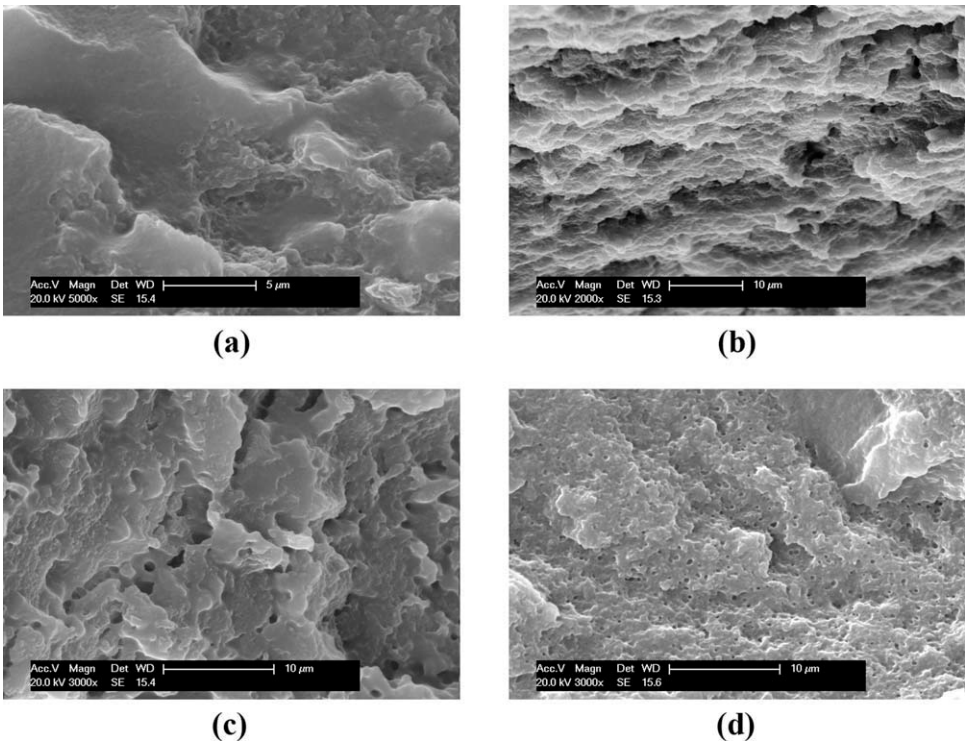

Figure 4. SEM photographs of cross-section of MILMs with (a) 10% NaCl, (b) 10% glucose, (c) 10% urea, and (d) 10% PEG300 as porogen. In all of these MILMs, BA/MMA in shell composition is 4/1.

Table II. Effects of Different Types of Porogen on the Adsorption Capacity, Permeation Amount, and Separation Factor by MILM

	Q (μmol/g)			P (mmol/m²)		
Porogen	L-Trp	L-Tyr	α	L-Trp	L-Tyr	β
NaCl	9.17	5.85	1.58	7.20	5.50	1.31
Glucose	28.53	3.46	9.06	5.94	4.57	1.30
Urea	13.88	6.75	2.09	5.24	4.02	1.30
PEG300	21.18	5.54	3.91	3.99	3.08	1.29

in Table II, different porogens lead to a significant impact on the MILM specific adsorption performance, which is due to the difference in inner microstructure caused by different porogens, including pore number, pore size, specific surface area, and so on. The glucose-containing film reaches the maximum adsorption (28.53 μmol/g), just because it has relatively more developed inner surface than other MILMs (Figure 4). On the other hand, the NaCl-containing film with smooth surface and low porosity has the lowest adsorption (9.17 μmol/g). In addition, Table II reveals that the adsorption to L-Tyr is low and almost constant for different films. This can be explained that the spatial structure of L-Tyr does not match that of the imprinted sites, which results in no relation between the adsorption to L-Tyr and inner microstructure in different MILMs. So, the MILMs demonstrated weak binding to L-Tyr.

In addition, the permeation data in Table II indicates that the NaCl-containing film with smooth channels has the highest permeation amount toward L-Trp and L-Tyr, whereas the PEG300-containing film with closed cell structure has the lowest permeation amount. Contrary to α, however, the type of porogen has little effect on the permeation separation factor β, which is kept around 1.30.

Effects of Shell Composition

A MILM was formed from the core-shell latex particles through the process of consolidation, compaction, deformation, and polymer chain inter-diffusion. The hard cores disperse homogeneously in the film to improve the mechanical strength, and the soft shells fuse to form a continuous phase. The composition of soft shell is apparently important to the inner structure of latex film and affects the recognition performance of MIP.

Adsorption in MILM is controlled by structural and chemical characteristics such as free volume, crystallinity, polarity, tacticity, crosslinkage, chain stiffness, presence of additives, etc.[18] The change of shell composition affects the free volume and stiffness of MILM. Lowering the content of BA or adding crosslinking agent restricts the movement of the polymer chains in MILM and reduces the free volume. In this study, the molecularly imprinted layer is modified on the surface of core-shell particles. The MIP layer is highly crosslinked so that the specific binding sites cannot be affected during the MILM-forming process or the inter-diffusion of chains in shell when exposed at room temperature. Some specific binding sites embedded excessively, however, cannot realize their interaction with template. If the chain segment motion was impetuous, the embedded sites might be exposed and the sites being ready to rebind template could be renewed. Then, the adsorption of MILM to template would increase.

Table IV. Effects of Soft Shell Composition on the Permeation Amount by MILM

	P (mmol/m²)	
BA/MMA	L-Trp	L-Tyr
4/1	5.94	4.57
2.5/2.5	3.27	2.46

The effects of BA/MMA ratio on the adsorption and separation properties of MILM were investigated, when the composition and dosage of molecularly imprinted layer were fixed. It is shown in Table III (No. 1 and No. 2) that the MILM with a higher BA/MMA ratio (No. 1) has a higher adsorbability. This can be explained that increasing the BA content increases the inter-diffusion of chains in shell, which renews the imprinted sites and improves the absorption amount. The permeation separation experiments (Table IV) show that the higher BA/MMA ratio, the higher permeation amount. This further proved that increasing the inter-diffusion of chains in shell renews the imprinted cavities and helps the template to pass during the process of permeation.

On the other hand, the adsorption to L-Tyr also increases with BA/MMA ratio increasing and leads to the decrease of separation factor α. Just as shown in Table III, almost all of the MILM with different content of porogen (5%–20% in mass fraction) conform to this trend.

Similarly, the influence of adding crosslinking agent or not on MILM adsorption performance was investigated (as shown in

Table III. Effects of Shell Composition on the Adsorption Capacity and Separation Factor by MILM

	Q (μmol/g)								
	L-Trp			L-Tyr			α		
Glucose content (% w/w)	1	2	3	1	2	3	1	2	3
5	8.62	6.43	5.81	4.58	2.89	2.34	1.90	2.25	2.50
10	12.83	12.09	8.92	4.31	2.61	0.99	3.06	4.78	9.22
15	6.87	10.14	4.39	2.71	3.03	2.69	2.57	3.44	1.64
20	10.13	9.75	12.04	4.05	3.26	2.85	2.56	3.07	4.32

The composition of shell in No. 1 is BA/MMA = 4/1, No. 2 is BA/MMA = 2.5/2.5, No. 3 has the same BA/MMA ratio as No. 1, but with additional 5% EGDMA as crosslinker. In all of these MILMs, glucose is used as porogen and its content is 10%.

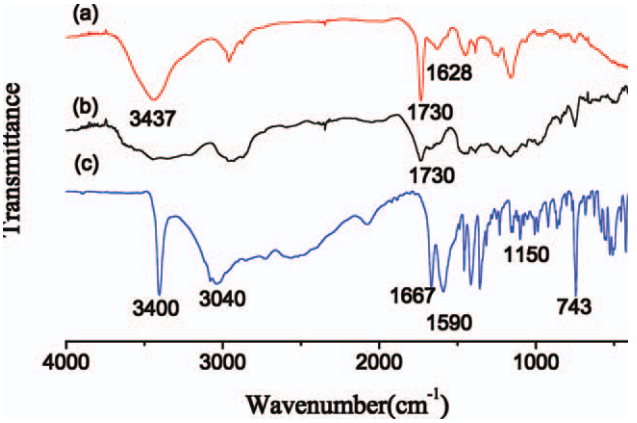

Figure 5. FTIR spectra of (a) MILM after adsorbing L-Trp, (b) MILM before adsorbing L-Trp, (c) L-Trp. In preparation of MILM, glucose content is 10%, BA/MMA in shell is 4/1. [Color figure can be viewed in the online issue, which is available at wileyonlinelibrary.com.]

Table III, No. 1 and No. 3). The addition of crosslinker (No. 3) limits the motion of chain segment and leads to the failure in exposing the recognition sites embedded excessively. So, the adsorption amount of MILM decreases.

FTIR Spectra of MILM

Figure 5 shows FTIR spectra of the porous MILM after (a) and before (b) adsorbing L-Trp and L-Trp (c). As in Figure 5(c), the peaks of N–H stretching vibration at 3400 cm^{-1} and in-plane bending vibration at 1590 cm^{-1}, and O–H stretching vibration in COOH groups at 3040 cm^{-1} are found. The peaks at 1460 cm^{-1}, 1150 cm^{-1}, 743 cm^{-1} are assigned to the skeleton vibrations, in-plane and out-plane bending vibration in aromatic rings. There is no obvious characteristic peaks of L-Trp in Figure 5(b), which indicates that no template was left after extraction, except the peak of C=O stretching vibration at 1730 cm^{-1}. After adsorbing L-Trp, it is found in Figure 5(a) that the characteristic peaks of the N–H groups in L-Trp shift from 3400 cm^{-1} and 1590 cm^{-1} to 3437 cm^{-1} and 1628 cm^{-1}, due to the interaction between N–H groups in L-Trp and $CONH_2$ groups in MILM. On the other hand, O–H stretching vibration in COOH groups also shifts from 3040 cm^{-1} to 2950 cm^{-1}, which suggests that hydrogen bonds are formed between COOH in L-Trp and $CONH_2$ in MILM.

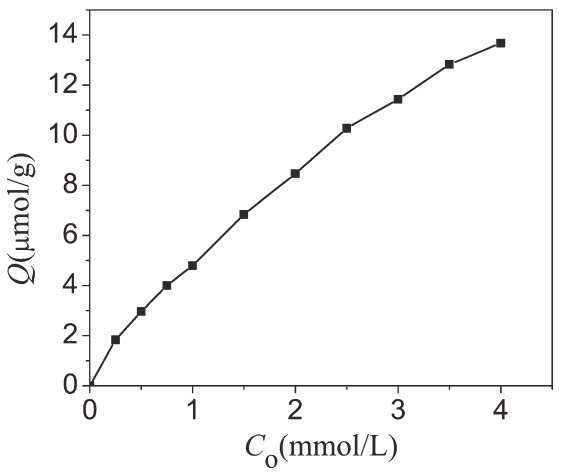

Figure 6. Binding isotherm of L-Trp onto MILM at 25°C.

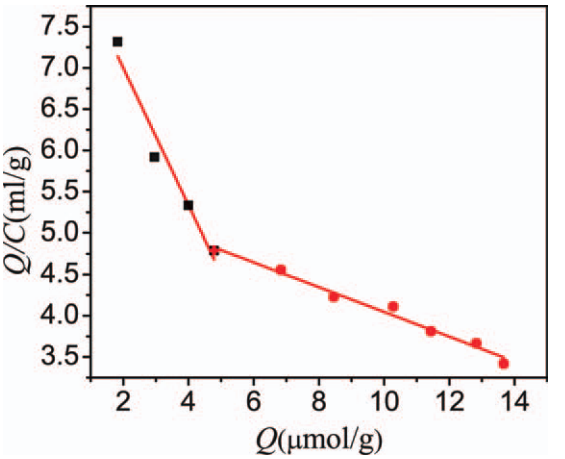

Figure 7. Scatchard plots for L-Trp onto MILM at 25°C. [Color figure can be viewed in the online issue, which is available at wileyonlinelibrary.com.]

Scatchard Analysis

A series of aqueous solutions of L-Trp were prepared at various concentrations, ranging from 0.05 to 4.0 mmol/L, to study the binding characteristics of MILM to template. The MILM with 10% glucose as porogen and BA/MMA = 4/1 in shell composition was chosen. The equilibrium binding isotherm is shown in Figure 6. The increase of L-Trp bound is observed due to the presence of the imprinted sites, a steric complementary shape to the template. To investigate further the binding ability of the MILM, Scatchard analysis is used to estimate the binding parameters as follows:

$$\frac{Q}{C} = \frac{Q_{max} - Q}{K_d} \tag{6}$$

where K_d was the equilibrium dissociation constant of binding sites (mmol/L); Q_{max} was the maximum apparent adsorption capacity of binding sites (μmol/g). As presented in Figure 7, Q/C is plotted against Q. The relation between Q/C and Q is distinctly nonlinear. Two regions for straight line are obtained, indicating that there exist two classes of nonequivalent binding sites. The equilibrium dissociation constant and maximum apparent adsorption capacity of the lower affinity binding sites determined from the straight area of the plot with C ranging from 0.25 to 1.0 mmol/L are 6.66 mmol/L and 37.0 μmol/g, respectively. For the higher affinity binding sites, with C ranging from 1.0 to 4.0 mmol/L, they are 1.20 mmol/L and 10.4 μmol/g, respectively.

CONCLUSIONS

A new type of self-supported porous MILM, exhibiting good recognition behavior towards L-Tryptophan in water media, was prepared by core-shell emulsion. The content and type of porogen and shell composition have crucial influence on the structure of MILM and, as a consequence, on the adsorption

capacity, permeability, and separation ability. Even if the permselective properties of MILM have to be improved, the high affinity towards template together with easy preparation and pollution-free provides a good basis for application in separation. Further research will be carried out for better separation of template molecules from mixed solution.

ACKNOWLEDGMENTS

This work was supported by the Program for New Century Excellent Talents in Fujian Province University (HX2006-102) and the Fujian Province Natural Science Foundation of China (2010J01037).

REFERENCES

1. Vlatakis, G.; Andersson, L. I.; Muller, R. *Nature* **1993,** *361*, 645.
2. Piletsky, S. A.; Dubey, I. Y.; Fedoryak, D. M.; Kukhar, V. P. *Biopolym. Kletka.* **1990,** *6*, 55.
3. Mathew-Krotz, J.; Shea, K. J. *J. Am. Chem. Soc.* **1996,** *118*, 8154.
4. Sergeyeva, T. A.; Piletsky, S. A.; Piletska, E. V.; Turner, A. P. F. *Macromolecules* **2003,** *36*, 7352.
5. Ulbricht, M. *J. Chromatogr. B* **2004,** *804*, 113.
6. Yoshikawa, M.; Fujisawa, T.; Izumi, J.-I.; Kitao, T.; Sakamoto, S. *Anal. Chem. Acta* **1998,** *365*, 517.
7. Yoshikawa, M.; Izumi, J. I. *Macromol. Biosci.* **2003,** *3*, 487.
8. Wang, H. Y.; Kobayashi, T.; Fukaya, T.; Fujii, N. *Langmuir* **1997,** *13*, 5396.
9. Kobayashi, T.; Wang, H. Y.; Fujii, N. *Anal. Chim. Acta* **1998,** *365*, 81.
10. Dzgoev, A.; Haupt, K. *Chirality* **1999,** *11*, 465.
11. Piletsky, S. A.; Matuschewski, H.; Schedler, U. *Macromolecules* **2000,** *33*, 3092.
12. Hilal, N.; Kochkodan, V. *J. Membr. Sci.* **2003,** *213*, 97.
13. Araki, K.; Maruyama, T.; Kamiya, N.; Goto, M. *J. Chromatogr. B* **2005,** *818*, 141.
14. Zhu, X. L.; Su, Q. D.; Cai, J. B.; Yang, J.; Gao, Y. *J. Appl. Polym. Sci.* **2006,** *101*, 4468.
15. Wang, J.-Y.; Liu, F.; Xu, Z.-L.; Li, K. *Chem. Eng. Sci* **2010,** *65*, 3322.
16. Tzitzinou, A. *Macromolecules* **2000,** *4*, 2695.
17. Stewarda, P. A.; Hearna, J.; Wilkinson, M. C. *Adv. Colloid Interface Sci.* **2000,** *86*, 195.
18. Nestorsona, A.; Leufvéna, A.; Jänström, L. *Polym. Test.* **2007,** *26*, 916.